CNRS
Centre National de la Recherche Scientifique

INFN
Instituto Nazionale di Fisica Nucleare

Notes on single-pole cavity approximation and long-wavelength interferometer approximation

L. Rolland

DRAFT

December 1, 2015

VIRGO * A joint CNRS-INFN Project
Project office: Traversa H di via Macerata - I-56021 S. Stefano a Macerata, Cascina (PI)
Secretariat: Telephone (39) 50 752 521 – Fax (39) 50 752 550 – e-mail virgo@pisa.infn.it

Contents

1 Introduction

The intial Virgo and LIGO $h(t)$ reconstructions are based on two important approximations: on one hand, the interferometer is assumed to have a size negligible with respect to the wavelength of the gravitational waves (long wavelength approximation) and on the other hand, the optical response of the arm Fabry-Perot cavities is approximated by a simple pole. Both approximations have non negligible errors compared to the calibration uncertainties, but the errors closely cancels when combining both, and the final {calibration + analysis} errors are quite small.

In this note, the two approximations are first described independently and the errors due to each approximation are estimated. Then the errors introduced when combining both approximation are estimated. Finally, some ideas about the use of these approximations for advanced detectors are given.

Other documents about similar topics can be found in [1, 2, 3, 4].

2 Response of the detector to GW's: long-wavelength approximation

The response of the interferometer to GW's is called the antenna response. It depends on the frequency of the GW and of the direction of the GW source with respect to the detector. Being dependeng on the source direction, this response cannot be included in the calibration and $h(t)$ reconstruction, but is taken into account in the different data analysis pipelines.

In the long-wavelength approximation, the frequency dependence is neglected and the response at $f = 0$ is used for all frequencies (up to few kHz). In this section, the antenna response is estimated for a Michelson interferometer with kilometer scale. The presence of Fabry-Perot cavities in the arm is taken into account in the next section.

Computation of the antenna response, with and without this approximation, have been described in [2]. The differential arm length induced by the a passing GW is written:

$$\tilde{V}(f) = \tilde{G}_+(\vec{n}, f)\, \tilde{h}_+(f) \;+\; \tilde{G}_\times(\vec{n}, f)\, \tilde{h}_\times(f) \tag{1}$$

where $\tilde{G}_+(\vec{n}, f)$ and $\tilde{G}_\times(\vec{n}, f)$ are the responses of the detector to the two polarizations of the wave.

In the case of the long wavelength approximation, $\tilde{G}_A(\vec{n}, f)$ is replaced by

$$F_A(\vec{n}) = \tilde{G}_A(\vec{n}, 0) \qquad (\text{with } A = +, \times) \tag{2}$$

$\tilde{G}_A(\vec{n}, f)$ is a complex number while $F_A(\vec{n})$ is a real number.

From $F_+(\vec{n})$ and $F_\times(\vec{n})$, one can compute the parameter $R_{det}(\vec{n})$ which is proportional to the range of the interferometer in the direction $\vec{n}$ assuming that the incicent GW wave contains

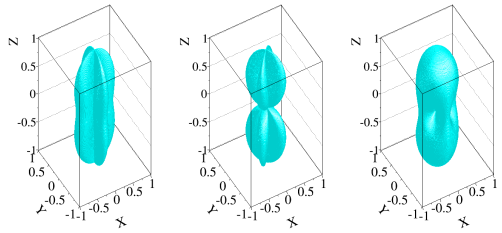

(a) 0 Hz (long wavelength approximation) (Virgo)

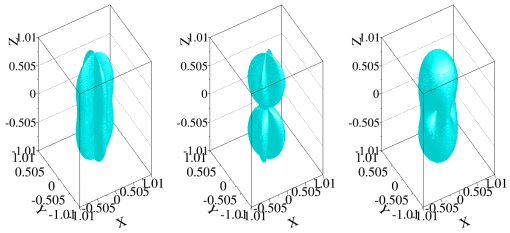

(b) 10 kHz (maximum Nyquist frequency of $h_{rec}(t)$) (Virgo)

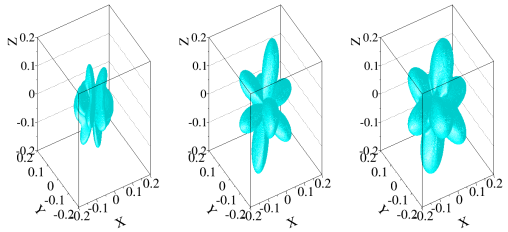

(c) 50 kHz (free spectral range of the Fabry-Perot cavity of Virgo)

Figure 1: Antenna response of an interferometer (3-km long arms) at different frequencies of GWs Left : response to the + polarization: G_+. Centre : response to the × polarization: $G_\times$. Right : response to a GW with both polarizations: R_{det}.

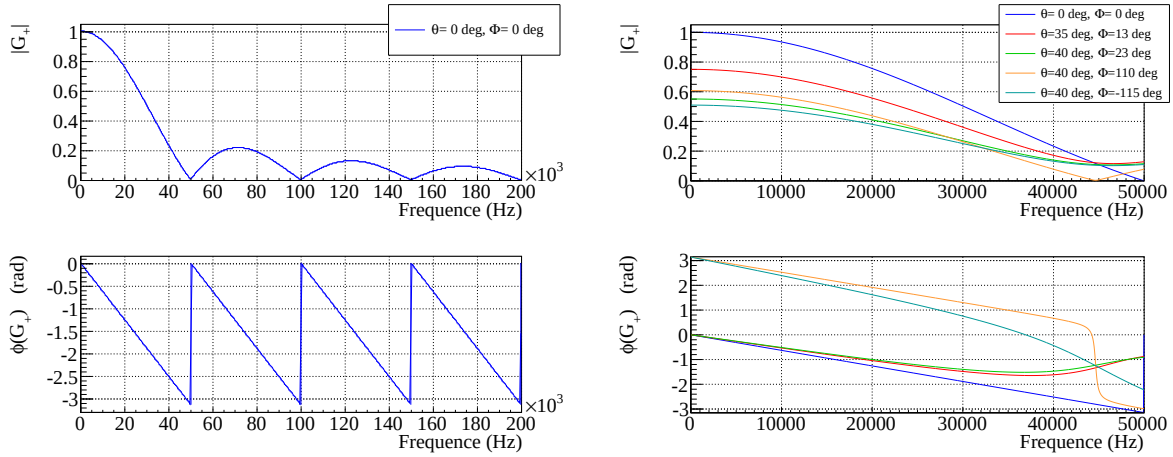

(a) Response G_+ at zénith from 0 to 200 kHz (Virgo) (b) Response G_+ in different sky directions, from 0 to 50 kHz (Virgo)

Figure 2: Interferometer antenna response $G_+(\vec{n}, f)$ as a function of the frequency f of the GW in different directions around the detector (3-km long arms).

both polarizations with the same amount $\iota = 0$:

$$R_{det}(\vec{n}) = \sqrt{\frac{1}{4}F_+^2(\vec{n})\left(1+\cos^2\iota\right)^2 + F_\times^2(\vec{n})\,\cos^2\iota} \quad (3)$$

$$= \sqrt{F_+^2(\vec{n}) + F_\times^2(\vec{n})} \quad (4)$$

The antenna response to the two polarizations in the detector referential, with x and y being along the interferometer arms, are shown in figure 1(a) for $f = 0$ (long wavelength approx.). In 3D, only the modulus of $\tilde{G}_A(\vec{n}, f)$ is shown. The responses at 10 kHz nd 50 kHz are also shown for comparison. The response at 10 kHz is not very different from the one at null frequency; on the contrary, the response at 50 kHz is very different, both in shape and in amplitude.

The variation of the detector response (amplitude and phase) with frequency f of the GW is better seen on figure 2 : $G_A(\vec{n}, f)$ is given as a function of f for some sky directions $\vec{n}$. The antenna response varies differently, both in amplitude and in phase, in different sky directions. Using the long wavelength approximation induces errors which depend both on the frequency and on the direction of the GW source in the sky with respect to the detector orientation.

In order to estimate the errors in all the directions due to the long wavelength approximation, the antenna response (module and phase) are represented in 2D in the plane (θ, ϕ) (θ is

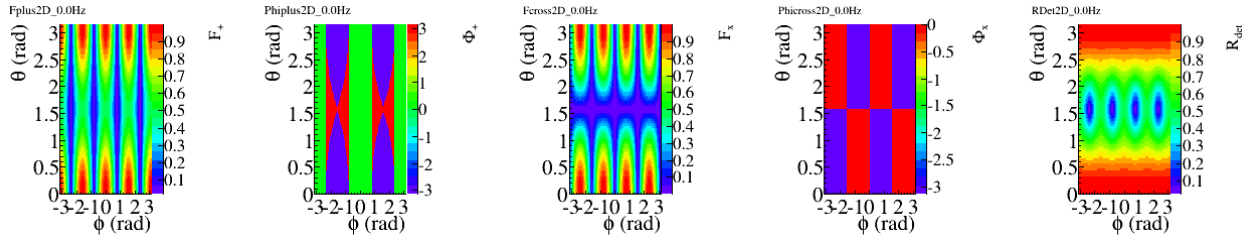

(a) Antenna response at $f = 0$, as a function of the sky direction (Virgo)

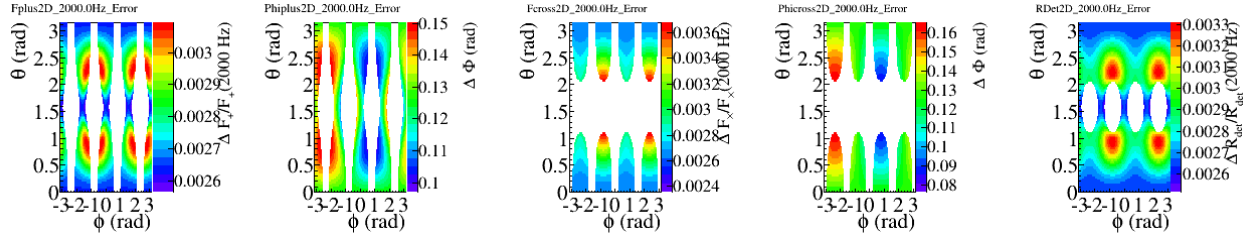

(b) Difference between the antenna responses at 2 kHz and 0 kHz, as a function of the sky direction (Virgo)

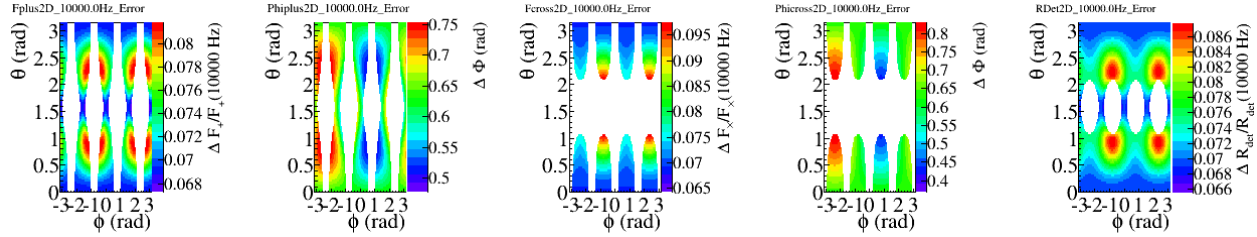

(c) Difference between the antenna responses at 10 kHz and 0 kHz, as a function of the sky direction (Virgo)

Figure 3: Comparison of the antenna responses at 2 kHz and 10 kHz with the response at $f = 0$ as a function of the sky direction (θ, ϕ) for an interferometer with 3-km long arms. The antenna response at $f = 0$ is given in the first line. The other two lines give the residuals between the response at 2 kHz (resp. 10 kHz) and the response at $f = 0$. Residuals (color scale) are $\frac{G_A(\vec{n},0)-G_A(\vec{n},f)}{G_A(\vec{n},f)}$ for the amplitude and $\phi(G_A(\vec{n},0)) - \phi(G_A(\vec{n},f))$ for the phase. They are calculated only for the sky directions where the antenna response is high enough, representing 95% of the observable volume (residuals are set to 0 at the positions where the detector sensitivity is smaller). Columns 1 and 2: amplitude and phase of G_+ ; Columns 3 and 4: amplitude and phase of $G_\times$; Column 5: amplitude of R_{det}.

the zenithal angle ; ϕ is the angle between the x axis and the projection of the source onto the plane (x, y)). In this plane, the difference between the exact response and the approximate response can also be shown. In the figure 3, the second and third lines show the ratio of the amplitudes $\frac{G_A(\vec{n},0)-G_A(\vec{n},f)}{G_A(\vec{n},f)}$ and the phase difference $\phi(G_A(\vec{n},0)) - \phi(G_A(\vec{n},f))$ between the response at 2 kHz or 10 kHz and the response at null frequency. The residuals are interesting only in the sky directions where the detector is sensitive enough to GW's. A minimum threshold

on the antenna response has been applied in order to show the residuals in 95% of the volume reachable by the detector[1]

In amplitude, the residuals are low, between 0.2% and 0.4% at 2 kHz, but increase to between 7% and 10% at 10 kHz, depending on the source direction.

In phase,, the residuals increase linearly with frequency, with a maximum going from 160 mrad at 2 kHz up to 800 mrad at 10 kHz. Below 10 kHz, this variation is almost linear (see figure 2). We can thus estimate a delay equivalent to this variation: the errors from the long-wavelength approximation are between 8 µs and 13 µs depending on the source direction. We have to highlight that the positions where this error is maximum are the positions where the detector sensitivity are the lowest, while the error stays close to 0 in the directions where the sensitivity is maximum.

For LIGO, with 4-km long arms, the errors from the long wavelength approximation are slightly higher (see figure 7). The amplitude errors are between 0.4% and 0.6% at 2 kHz and between 13% and 18% 10 kHz. The timing errors are between 10 µs and 18 µs depending on the source direction.

[1] thresholds of 0.47, 0.458 and 0.445 for the antenna responses at 0 Hz, 2 kHz and 10 kHz respectively.

3 Optical response of the Fabry-Perot cavities: single-pole approximation

Optical responses of the Fabry-Perot cavity to both a passing GW and a moving mirror of the cavity have been computed in [2].

3.1 Exact optical cavity response

3.1.1 Response to a gravitational wave

The exact response to a GW is described as a function of the GW frequency f by:

$$C(f) \;=\; \frac{1 - r_1 r_2}{1 - r_1 r_2 \mathrm{e}^{-\mathrm{j}4\pi f T}} \tag{5}$$

where r_1 and r_2 are the amplitude reflection coefficients of the cavity mirrors, and $T = \frac{L_0}{\mathrm{c}}$ where L_0 is the cavity length.

3.1.2 Response to the motion of a cavity mirror

In the case of a length variation due to mirror displacements x_{in} et x_{end}, the cavity response is:

$$V(f) = \frac{2}{L_0}\, C(f)\, \left[\mathrm{e}^{-\mathrm{j}2\pi f T} x_{end}(f) \;-\; x_{in}(f)\right] \tag{6}$$

The shape of the optical response is the same than the one to a GW, but with some additional delay when the end mirror is moving.

3.2 Single-pole approximation

For initial GW detectors, the frequency dependence of the cavity response has been approximated by a simple pole at f_p in the $h(t)$ reconstruction process:

$$C_{pole}(f) \;=\; \frac{1}{1 + \mathrm{j}\frac{f}{f_p}} \tag{7}$$

where $f_p == \frac{\mathrm{c}}{4\mathcal{F}L_0}$ and the arm cavity finesse is $\mathcal{F} = \frac{\pi\sqrt{r_1 r_2}}{1 - r_1 r_2}$.

The Advanced Virgo ($\mathcal{F} = 450$) exact optical response is shown in blue in the figure 4 and the approximation by a simple pole is shown in red. Amplitude and phase residuals are shown on the right panels. Errors in modulus and phase due to the approximation increase with frequency, Modulus errors are of 0.5% and 11% at 2 kHz and 10 kHz. The phase error is proportional to the frequency and is thus equivalent to a delay: using the simple pole introduces an error of $\sim -13\,\mu\mathrm{s}$.

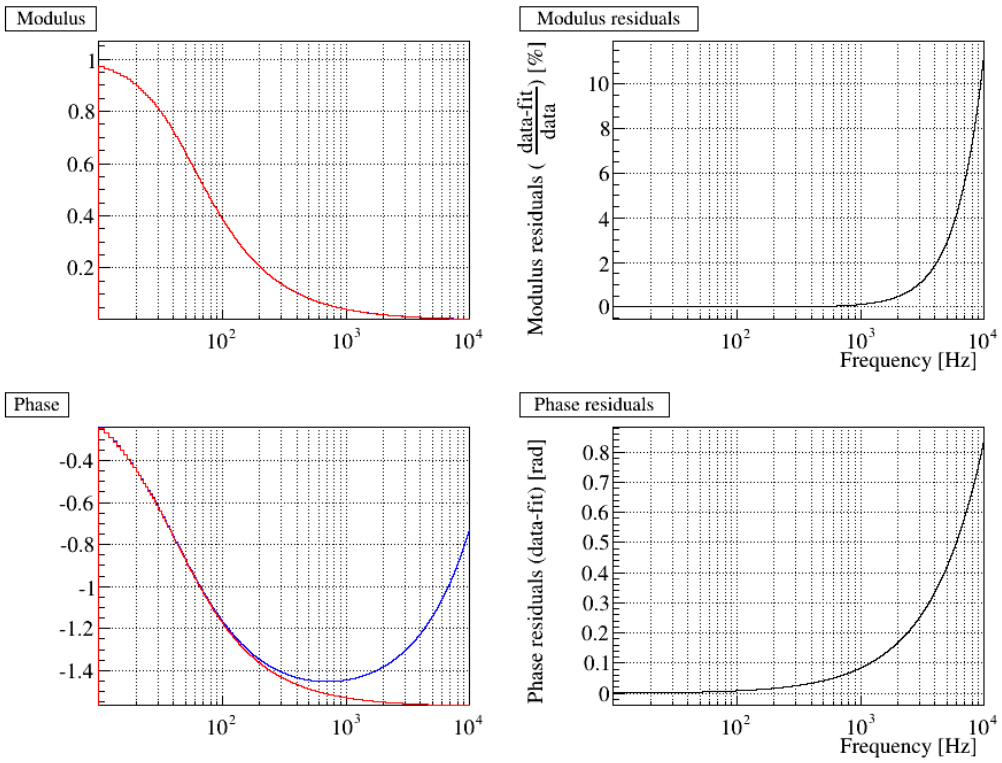

Figure 4: Optical response of ac cavity with finesse $\mathcal{F} = 450$ (Advanced Virgo). Left: module and phase of the exact response (blue) and of the single pole approximation (red). Right: residuals in modulus and phase of the approximation compared to the exact response.

4 Combination of both approximations

The full response of the detector is the combination of both responses to a GW: response of the optical cavities and response of the interferometer.

In order to extract the errors introduced by the combination in the complete pipeline {calibration + data analysis}, one has to compare the exact response $G_A(\vec{n}, f)\, C(f)$ to the approximated response $G_A(\vec{n}, 0)\, C_{pole}(f)$.

In order to compare the combination of both approximations to the exact detector response to GWs, the following residuals have been computed:

$$\begin{aligned} \text{in modulus} \quad &: \quad \frac{G_A(\vec{n}, 0) \times C_{pole}(f) - G_A(\vec{n}, f) \times C(f)}{G_A(\vec{n}, f) \times C(f)} \\ \text{in phase} \quad &: \quad \phi\Big(G_A(\vec{n}, f = 0) \times C_{pole}(f)\Big) \; - \; \phi\Big(G_A(\vec{n}, f) \times C(f)\Big) \end{aligned} \tag{8}$$

Such residuals are shown for Advanced Virgo as a function of frequency in figure 5, for some directions of the GW around the detector. The residuals computed at 2 kHz and 10 kHz are shown as a function of the sky direction in the figure 6. Since the phase residuals are linear as a function of frequency, they have been converted into an equivalent delay in this figure.

These results confirm that the errors introduced by the combination of both approximations are low. In amplitude, the errors stay below 0.1% at 2 kHz and below 2.5% at 10 kHz. In phase, the errors converted into a delay are in the range $\pm 3\,\mu$s depending on the sky direction around the detector.

For Advanced LIGO (see figure 8), the amplitude errors stay below 0.2% at 2 kHz and below 4.5% at 10 kHz ; In phase, the errors converted into a delay are in the range $\pm 4\,\mu$s depending on the sky direction around the detector.

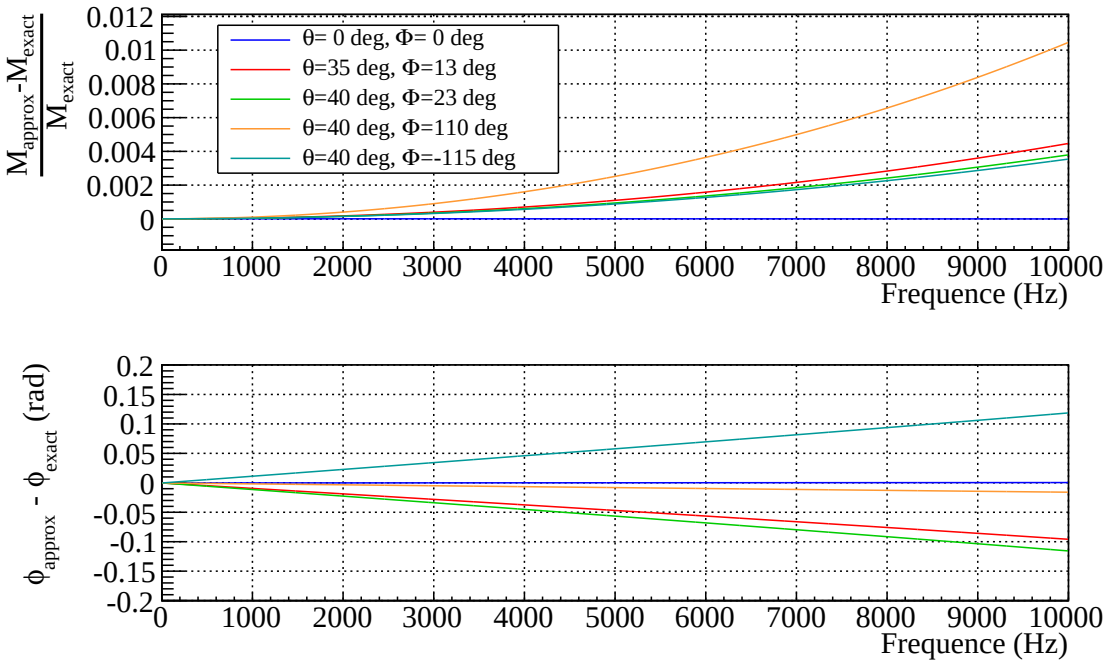

Figure 5: Comparison of the combination of both approximations with the exact response for Advanced Virgo: the residuals (see definition in equation 8) as a function of the frequency for some sky directions (θ, ϕ).

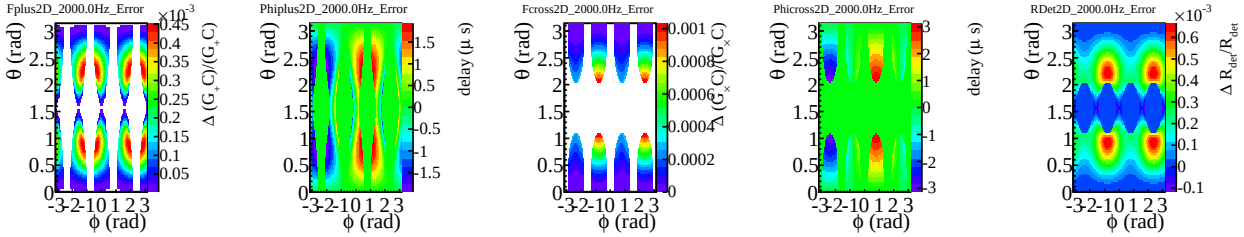

(a) Difference between the full responses at 2 kHz and 0 Hz, as a function of the sky direction (AdV)

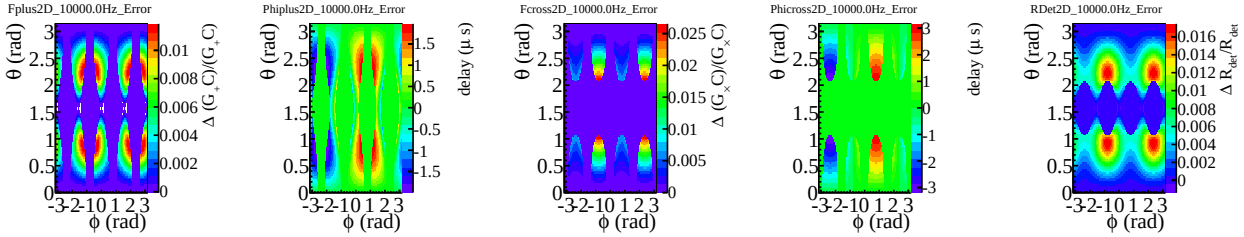

(b) Difference between the full responses at 10 kHz and 0 Hz, as a function of the sky direction (AdV)

Figure 6: Comparisons of the combination {antenna response × response of optical cavities} at 2 kHz and 10 kHz with the combination {antenna response at $f = 0$ × simple pole} as a function of the direction in the sky (θ, ϕ) (case of Advanced Virgo). Each line gives the residuals between the response at 2 kHz (resp. 10 kHz) and the response at $f = 0$. The residuals (scale colors) are $\frac{G_A(\vec{n},0)\times C_{pole}(f) - G_A(\vec{n})\times C(f)}{G_A(\vec{n},f)\times C(f)}$ for the amplitude and $-\frac{\phi(G_A(\vec{n},0)\times C_{pole}(f)) - \phi(G_A(\vec{n},f)\times C(f))}{2\pi f}$ for the delay. They are calculated only for the most sensitive directions, where the antenna response is high enough, representing 95% of the observable volume (residuals are set to 0 at the positions where the detector sensitivity is smaller) Columns 1 and 2: amplitude and delay for a wave with + polarization ; Columns 3 and 4: amplitude and delay for a wave with × polarization ; Column 5: amplitude of R_{det}.

5 My conclusions about what models to be used for advanced detectors?

Each approximation induces important errors on the reconstructed $h(t)$ signal, but, fortuitously, the use of both approximations results in small errors. The errors on the amplitude of $h(t)$ increase with the frequency but had a very low contribution to the calibration error budget for initial Virgo and LIGO. The errors on the phase can be approximated by a delay, being in the range $[-3; +3]$ µs depending on the sky direction. This was not negligible, contributing to about a third of the timing error budget of the initial detectors. These errors were included in the calibration systematic uncertainties for the initial detectors.

For advanced detectors, the antenna response are not changed (the arm lengths do not change), but the optical responses are modified since the finesse of the cavities are higher. The comparison of the combination of both models up to 10 kHz with the AdVirgo parameters shown in this note (figure 5) give similar results: the combination of both approximations results in small errors for AdVirgo also. At 10 kHz, the errors are at maximum 2.5% in amplitude. Errors in phase/timing are ± 3 µs (the errors depend on the source direction with respect to the interferometer).
Advanced LIGO has the same finesse as Advanced Virgo but longer arms. It results is slightly larger errors due to the approximations: 4.5% in amplitude at 10 kHz and ± 4 µs in timing.

For advanced detectors, we will have to choose between:

1. using both approximations, as for the initial detectors,
2. using both the exact responses,
3. using both approximations, plus some timing corrections for the residual bias (to be done in the data analysis pipelines),
4. using the exact cavity response (in the calibration) and the long-wavelength approximation (in the data analysis).

Option 1 looks a good enough solution and simple to setup in the different pipelines. It could be extended to **option 3** by adding, in the analysis pipelines, small corrections of a few microseconds in the different $h(t)$ time-series depending on the source direction. Biais due to the approximations would be lower than 0.2% (4.5%) in amplitude at 2 kHz (10 kHz), and timing errors lower than 1 µs could be easily achieved.

Option 2 would be more elegant, using both exact solutions instead of both approximations. The use of the exact Fabry-Perot cavity response is quite easy to insert in the calibration pipelines, but the exact antenna response is probably more difficult to setup in the different

data analysis pipelines: the $h(t)$ signals from the different detectors should be filtered through different transfer functions (instead of simple gains) for every detectors and every sky directions.

Option 4, using the exact cavity response and the approximate antenna response, would result in errors as the one shown in figures 2 and 3. Amplitude errors would not be important ($\sim 0.5\%$) below 2 kHz, but start being important for higher frequency searches ($\sim 10\%$ at 10 kHz). About timing errors, the absolute timing of the $h(t)$ channel would be offset, on average, by $\sim 10\,\mu s$ for Virgo data and $\sim 14\,\mu s$ for LIGO data. At first order, such average delays could be pre-corrected for in the $h(t)$ reconstruction pipelines. Additionnaly, as for option 1, option 4 could be extended by adding, in the analysis pipeline, small corrections of a few microseconds in the different $h(t)$ time-series depending on the source direction, reducing the timing bias to below $1\,\mu s$. But such solution would result in biais larger than with option 1 since the fortuitous cancelation of the amplitude errors would not be effective any more.

Practically, the optical response of the cavity is integrated in the $h(t)$ reconstruction, while the antenna response is used in the different data analysis pipelines since it depends on the source direction in the sky. That's why it is important that the groups taking care of the $h(t)$ reconstruction on one hand and the search groups on the other hand agree about the use or not of the two approximations and possible small timing corrections. Moreover, the analysis being common for Virgo and LIGO, the same models must be used in the (h) reconstruction and pipelines for all detectors.

As of today, my personal favorite option is the option 3: using both approximations, and adding small timing corrections for the antenna response as a function of the source direction for each detector. However, the presence of the signal-recycling cavity was not estimated in this note. Depending on its effect on the optical response of the detector, some other options might be chosen.

5.1 Some more remarks

As long as the long wavelength approximation is done, whatever the model used for the cavity response, the timing errors from the different detectors of the network will have the same difference ("time of flight"): so they will induce the same results and same errors on the sky localization. What will change depending on the cavity response model is the absolute timing of the GW event from the network, but probably $\sim 10\,\mu s$ error is not a big issue.

Using the long-wavelength approximation, errors on the time of flight of a GW event seen in different detectors are lower than $8\,\mu s$. Correcting for the direction-dependent few microseconds bias due to the approximation in the data analysis pipelines would reduce this error and improve the sky localization. But probably this bias is not currently the limiting factor on the sky localization.

A Some plots for the LIGO case

The following plots have been computed for an interferometer with 4-km long arms and a Fabry-Perot cavity with finesse $\mathcal{F} = 450$.

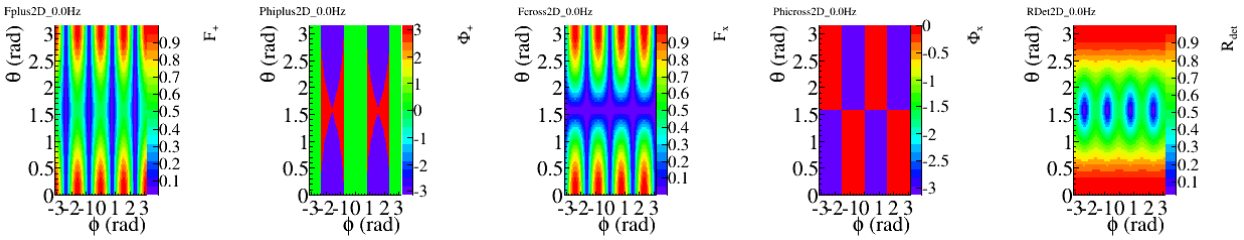

(a) Antenna response at $f = 0$, as a function of the sky direction (LIGO)

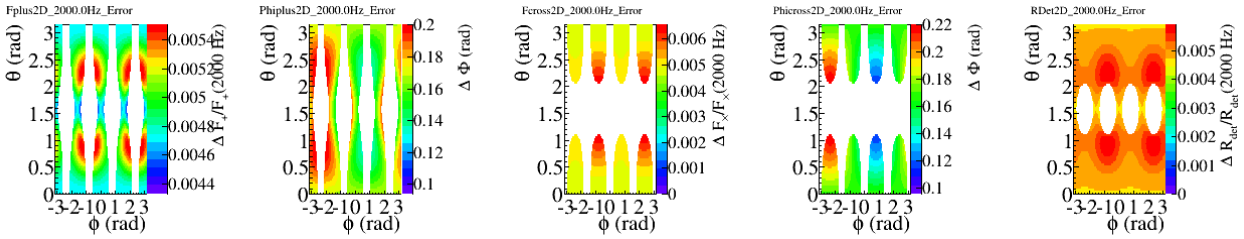

(b) Difference between the antenna responses at 2 kHz and 0 kHz, as a function of the sky direction (LIGO)

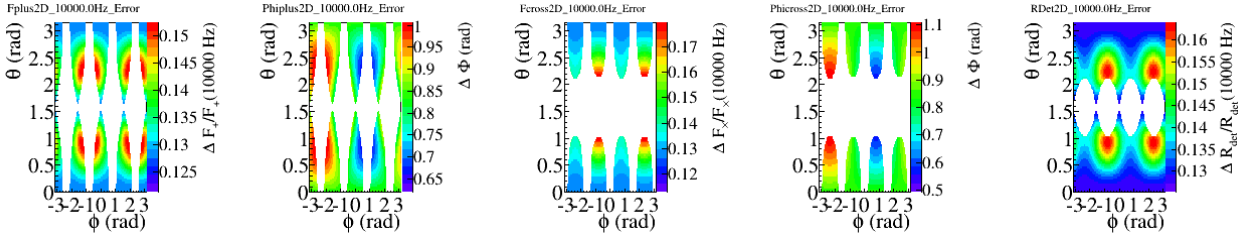

(c) Difference between the antenna responses at 10 kHz and 0 kHz, as a function of the sky direction (LIGO)

Figure 7: Comparison of the antenna responses at 2 kHz and 10 kHz with the response at $f = 0$ as a function of the sky direction (θ, ϕ) for an interferometer with 4-km long arms. The antenna response at $f = 0$ is given in the first line. The other two lines give the residuals between the response at 2 kHz (resp. 10 kHz) and the response at $f = 0$. Residuals (color scale) are $\frac{G_A(\vec{n},0) - G_A(\vec{n},f)}{G_A(\vec{n},f)}$ for the amplitude and $\phi(G_A(\vec{n},0)) - \phi(G_A(\vec{n},f))$ for the phase. They are calculated only for the sky directions where the antenna response is high enough, representing 95% of the observable volume (residuals are set to 0 at the positions where the detector sensitivity is smaller). Columns 1 and 2: amplitude and phase of G_+ ; Columns 3 and 4: amplitude and phase of $G_\times$; Column 5: amplitude of R_{det}.

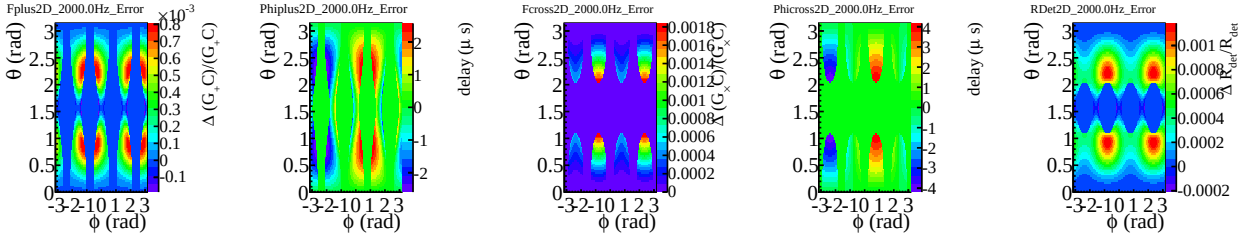

(a) Difference between the full responses at 2 kHz and 0 Hz, as a function of the sky direction (aLIGO)

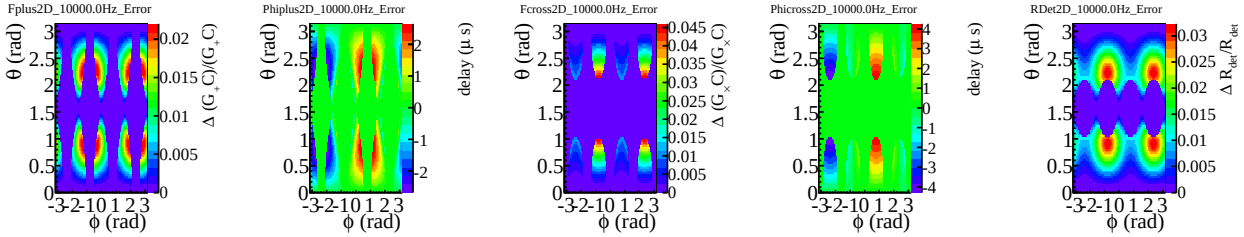

(b) Difference between the full responses at 10 kHz and 0 Hz, as a function of the sky direction (aLIGO)

Figure 8: Comparisons of the combination {antenna response × response of optical cavities} at 2 kHz and 10 kHz with the combination {antenna response at $f = 0$ × simple pole} as a function of the direction in the sky (θ, ϕ) (case of Advanced LIGO). Each line gives the residuals between the response at 2 kHz (resp. 10 kHz) and the response at $f = 0$. The residuals (scale colors) are $\frac{G_A(\vec{n},0)\times C_{pole}(f) - G_A(\vec{n})\times C(f)}{G_A(\vec{n},f)\times C(f)}$ for the amplitude and $-\frac{\phi(G_A(\vec{n},0)\times C_{pole}(f)) - \phi(G_A(\vec{n},f)\times C(f))}{2\pi f}$ for the delay. They are calculated only for the most sensitive directions, where the antenna response is high enough, representing 95% of the observable volume (residuals are set to 0 at the positions where the detector sensitivity is smaller) Columns 1 and 2: amplitude and delay for a wave with + polarization ; Columns 3 and 4: amplitude and delay for a wave with × polarization ; Column 5: amplitude of R_{det}.

References

[1] L. Savage *et al.*, *LIGO high-frequency response to length- and GW-induced optical path length variations*. G060667-x0, 2006.

[2] M. Rakhmanov *et al.*, "High-frequency corrections to the detector response and their effect on searches for gravitationnal waves," *Class. Quantum Grav.*, vol. 25, no. 184017, 2008. (arXiv:0808.3805).

[3] K. Kawabe, *Response of a Single Fabry-Perot Cavity*. T1000212-v1, 2010.

[4] K. Izumi, *Calibration meeting material: toward accurate DARM response modeling*. G1501316-v1, 2016.